



RESEARCH ARTICLE

EXPERIMENTAL AND NUMERICAL INVESTIGATION OF A DEFICIENT
STORMWATER DRAINAGE SYSTEM

Cem YILMAZER ^{1*} , Ahmet Ozan ÇELİK ² 

¹ Department of Civil Engineering, Faculty of Civil Engineering, Yıldız Technical University, Istanbul, Turkey

² Department of Civil Engineering, Faculty of Engineering, Eskişehir Technical University, Eskişehir, Turkey

ABSTRACT

In this paper, a deficient stormwater system was investigated with experimental and numerical methods. The main goal was to obtain an experimentally validated 3D computational fluid dynamics (CFD) model to identify the problems of the system and offer design solutions via numerical modeling. A scaled physical model of the structure was built for CFD validation. The validation was done via comparisons of point pressure statistics, discharge and water levels. Different mesh structures and turbulence closure methods were also tested for verification of the model. The validated model was then used to determine the cause of the problems in the structure. New geometries were tested numerically to suggest solutions to the detected problems. Empirical approaches and also regulations for the stormwater structures were also considered for comparison. Findings of this study suggest that a verified and validated CFD model is an effective tool to investigate special geometries for specific hydraulic structure problems where conventional approaches are insufficient.

Keywords: Stormwater drainage system, CFD, Hydraulic modelling, Validation

1. INTRODUCTION

Climate change, irregular urbanization and conurbation together with high intensity precipitations may cause extreme discharges which eventually need to be removed safely. In such cases, the existing stormwater drainage systems, if not effective enough, may be causing further problems. Although design and rehabilitation of such systems can be performed using experimental, empirical and theoretical approaches there are valuable results in the literature involving numerical modelling of stormwater drainage systems, some of which are reviewed below.

Saiyudthong and Guymer investigated joining pipes with different angles in a circular manhole under surcharge flow conditions reporting that increasing the angle between the pipes causes added momentum and decreases the energy loss coefficient in the manhole [1]. However, they were not able to obtain a good validation using experimental results. Zhao et al. simulated fully surcharged flow at a 90° combining sewer junction and found a good agreement between CFD and experiments for water depth, energy loss and velocity profiles [2]. Observing the flow inside a chute manhole, Sousa et al. focused on the effect of oxygen level on the flow characteristics as the hydraulic jump occurs. They measured velocity profiles, pressure at various locations and water levels for validation which lead to the conclusion that CFD can characterize water-air phase mixture reasonably well [3]. More recently, Beg et al. performed a CFD model study for both free surface flow and pressurized flow inside a manhole [4]. The numerical model was validated using 1:1 scaled experiments with different discharge combinations. However, they modeled a manhole with a simple geometry and this study did not include real flow cases or geometrical improvements.

*Corresponding Author: cem.yilmazer@yahoo.com

Received: 01.10.2022 Published: 28.03.2024

Although the literature has numerous examples of studies utilizing numerical methods, the ones listed so far do not involve detection of problems and/or providing solutions involving real cases using CFD tools. Studies involving more realistic cases are reviewed below.

Motlagh et al. investigated energy losses and flow behaviour in a more realistic model of a manhole with two inlet and one outlet pipe, reporting that increasing the height of the lateral inlet pipe causes energy loss coefficient to decrease as a result of decreasing eddy flow [5]. Chen et al. performed a CFD analysis for optimization of a municipal sewer system design aiming to optimize the design of an existing combined sewer system and the numerical model was validated using experimental results [6]. Isel et al. described a general method based on CFD to investigate discharge-water depth relationships for combined sewer overflow chambers, particularly for complex geometries. They reported problems with the validation due to sensors accuracy and complex geometry of the system [7]. Kaur, Laanearu and Annus in a case study analysed a pipe's performance between two manholes for design and storm discharges considering slurry flow. A three-phase CFD model was used, however without validation [8]. Beg, Carvalho and Leandro investigated an ideal manhole with CFD models testing three different chute manholes. This study resulted in the best design option based on hydraulic grade line and energy loss coefficient although the numerical model wasn't validated with experimental work [9].

Ozolcer and Dundar modeled flow with CFD in a half-bench manhole comparing three alternative manhole geometries for energy loss coefficients but they didn't validate the CFD model with experimental findings [10]. Beg, Carvalho and Leandro investigated a manhole with an integrated gully to the structure. CFD model was validated with 1:1 scaled experiments. They found that increasing the surcharge flow in the manhole decreased retention of stormwater in the gully and decreased the energy dissipation near the inlet [11]. Wang and Vasconcelos performed a CFD study for manhole cover displacement due to the release of entrapped air pocket inside the manhole considering rapid filling with stormwater as an operational problem [12]. Beg, Carvalho and Leandro more recently investigated numerically manhole structural mold shapes, small changes in inlet orientations and changes in the manhole to inlet pipe ratios for their effect on manhole head loss coefficient [13].

Literature suggests that CFD is a useful tool for many stormwater applications. However, the relevant studies in the literature, some of which have been given above either present unvalidated numerical models and/or use ideal systems not fully representing real cases. That is, the CFD method, proven to be very useful in hydraulics studies, seems to be not effectively used in providing solutions to the real hydraulic problems.

This study aims to address a practical concern in a given public stormwater drainage system, using the experimentally validated numerical models effectively to design new components/geometries in a stormwater system with known problems and also discuss shortcomings of the relevant regulations and empirical equations.

2. MATERIALS AND METHODS

2.1. The Investigated Structure

The drainage system investigated here is located in Eskisehir, Turkey and it involves a manhole and four integrated pipes (Figure 1). It was reported to the authors by the authorities that the manhole had conurbation related design and overflow problems. The main inlet pipe's diameter was changed from originally designed 1500 mm to 1200 mm to open space for a crossing heat pipeline. As a result, overflow and backflow occurred in the system. Subsequently, two additional pipes were integrated to the manhole as a solution. These pipes are 500 mm and 350 mm in diameters (Figure 1a, 1b) and are also believed to be causing backflow during extreme discharges.

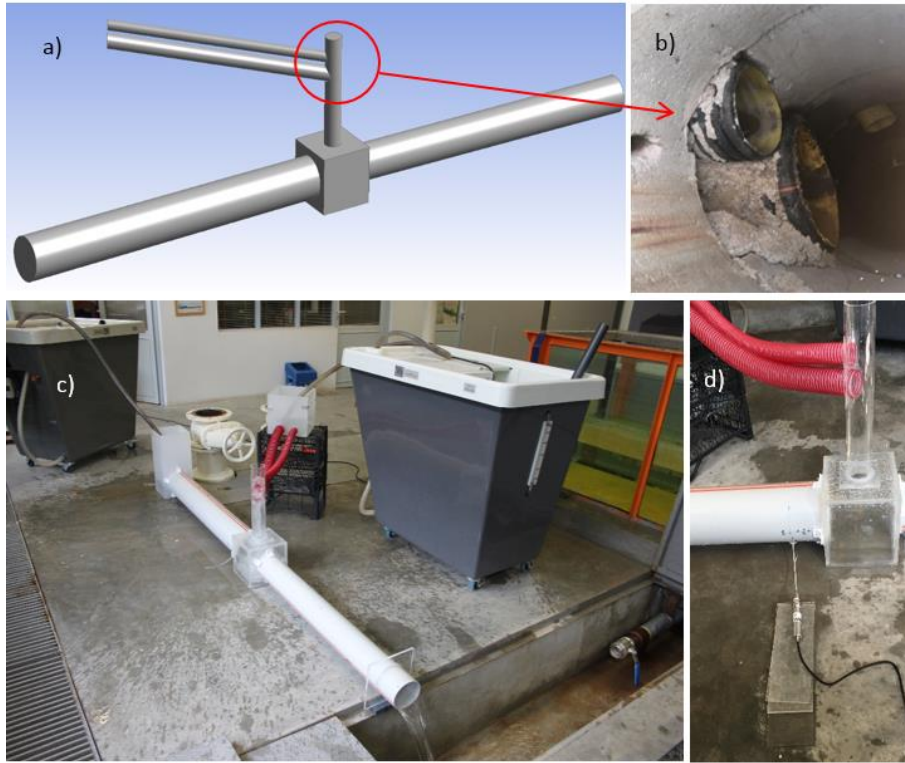


Figure 1. The manhole and four integrated pipes (a); integration of secondary corrugated pipes to the manhole in situ (b); the experimental set-up, general view (c); location of the pressure sensor (d)

2.2. The Physical Model

Experiments were performed at the Hydraulics Laboratory of the Eskişehir Technical University in Eskişehir, Turkey. The physical model was built with 1:10 geometric scale, to use the physical space in the current lab facilities effectively (Figure 1c, 1d). Froude dynamic similitude was used. Dimensions of the physical model are given in detail (Figure 2 and Tables 1, 2). For more about the experimental procedure please refer to Yilmazer [14].

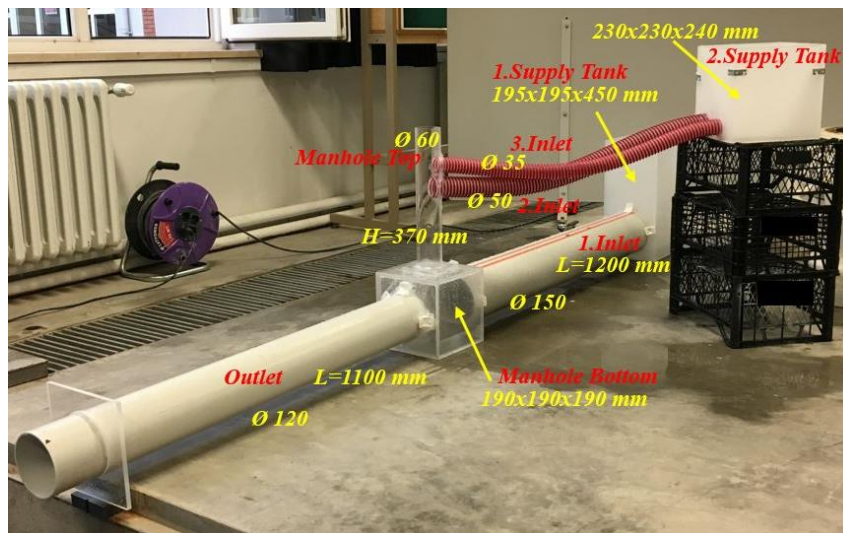


Figure 2. The experimental set-up with elements and dimensions

Table 1. The experimental set-up pipes dimensions

| Pipes | Diameter (mm) | Length (mm) | Slope (mm/mm) |
|-------------|---------------|-------------|---------------|
| Inlet 1 | 150 | 1200 | 0.0037 |
| Inlet 2 | 50 | 810 | 0.0158 |
| Inlet 3 | 35 | 810 | 0.17 |
| Outlet | 120 | 1100 | 0.09 |
| Manhole Top | 60 | 370 | --- |

Table 2. The experimental set-up elements dimensions

| Elements | Width (mm) | Length (mm) | Height (mm) |
|----------------|------------|-------------|-------------|
| 1. Supply Tank | 195 | 195 | 450 |
| 2. Supply Tank | 230 | 230 | 240 |
| Manhole Bottom | 190 | 190 | 190 |

90 different discharge combinations were generated for observing the outlet discharges of the system to investigate the system’s performance (Table 3). For this, stabilized water levels in the manhole and the first supply tank were measured for all 90 combinations. Five of the combinations also included detailed pressure measurements at a fixed point at the bottom of the first main inlet pipe, 100 mm near the manhole (Figure 1d). This point was specifically selected to obtain pressure data to be used for CFD validation. Omega PX409-10WG USBH type pressure sensor was used for measuring pressure. The DC off-set of the pressure sensor was measured and recorded before and after each set of experiments and the obtained data was corrected accordingly [14].

Table 3. Outlet Discharge for two inlet discharge combinations (l/s)

| Q ₁ \Q ₂ | 0.0 | 0.1 | 0.3 | 0.5 | 0.8 | 1.0 | 1.2 | 1.5 | 1.8 | 2.0 |
|--------------------------------|------|------|------|------|------|------|------|------|------|------|
| 0.1 | 0.10 | 0.19 | 0.36 | 0.58 | 0.79 | 0.82 | 1.04 | 1.32 | 1.58 | 1.82 |
| 0.3 | 0.29 | 0.39 | 0.54 | 0.75 | 1.02 | 1.04 | 1.25 | 1.48 | 1.75 | 1.98 |
| 0.5 | 0.49 | 0.57 | 0.79 | 0.97 | 1.11 | 1.22 | 1.45 | 1.74 | 1.92 | 2.22 |
| 0.8 | 0.78 | 0.86 | 1.04 | 1.29 | 1.52 | 1.54 | 1.67 | 1.79 | 2.08 | 2.63 |
| 1.0 | 0.99 | 0.87 | 1.07 | 1.25 | 1.56 | 1.75 | 1.96 | 2.30 | 2.67 | 2.71 |
| 1.2 | 1.18 | 1.03 | 1.25 | 1.43 | 1.71 | 1.87 | 2.17 | 2.22 | 2.50 | 2.90 |
| 1.5 | 1.50 | 1.32 | 1.67 | 1.82 | 2.08 | 2.11 | 2.38 | 2.67 | 2.78 | 3.18 |
| 1.8 | 1.80 | 1.63 | 1.83 | 2.15 | 2.27 | 2.35 | 2.63 | 2.94 | 3.08 | 3.36 |
| 2.0 | 2.00 | 1.85 | 2.06 | 2.17 | 2.41 | 2.67 | 2.94 | 3.13 | 3.33 | 3.44 |
| 2.5 | 2.50 | 2.20 | 2.41 | 2.50 | 2.86 | 3.03 | 3.28 | 3.51 | 3.70 | 4.17 |

Second discharge (total of 2nd and 3rd inlets) was limited to 2.0 l/s after which overflow occurred. Normally, secondary pipe’s design discharges should be 4.93 and 1.39 l/s respectively according to Manning equation (with a total capacity of 6.32 l/s). But this value was observed to be around 2.0 l/s during the experiments which show that the integrated secondary corrugated pipe causes the backflow effect.

Another investigation was about the case when the secondary pipes’ discharge (Q₂) is more than main pipe’s discharge (Q₁). In this case, backflow effect was seen in the first supply tank. This is presumably due to high turbulence levels in the manhole. Outlet discharge was observed to be decreasing compared to the inlet discharge as a result of the accumulation and backflow in the tank. Particularly, the difference is much more apparent when Q₂ is dominant [14].

2.3. The Numerical Model

With a separate but parallel effort, a multi-phase CFD model was built using ANSYS-CFX solver. CFD is a flow simulation methodology based on discretized (second order, transient, implicit schemes-backward Euler-, using trilinear interpolation approach with turbulence -high resolution- closures given in Table 2, for details of the numerical schemes please refer to ANSYS C. 2010, ANSYS C. 2013 [15,16] equations of continuity and momentum. All models employed a convergence criteria of 10^{-4} for mass and momentum equations. For more detail about the CFD basics, model verification/validation and free-surface modeling please refer to Chen et al. [6], Isel et al. [7], Beg, Carvalho and Leandro [4] and Yilmazer [14].

2.3.1. Verification

First, drawings of 1:10 scaled storm water system (domain) were generated (Figure 1a) with dimensions identical to that of the experiments. For mesh independency study to choose optimum mesh sizes, CFD models with 6 different mesh configurations were compared with experimental results (1.0-2.0 l/s discharge combinations, representing the upper and lower limits of the whole experiment). The mesh structures were classified as coarse (2), medium (1) and fine (3) and summarized along with the element sizes in Table 4. Figure 3 shows the domain with mesh elements as well as the regions with refined mesh.

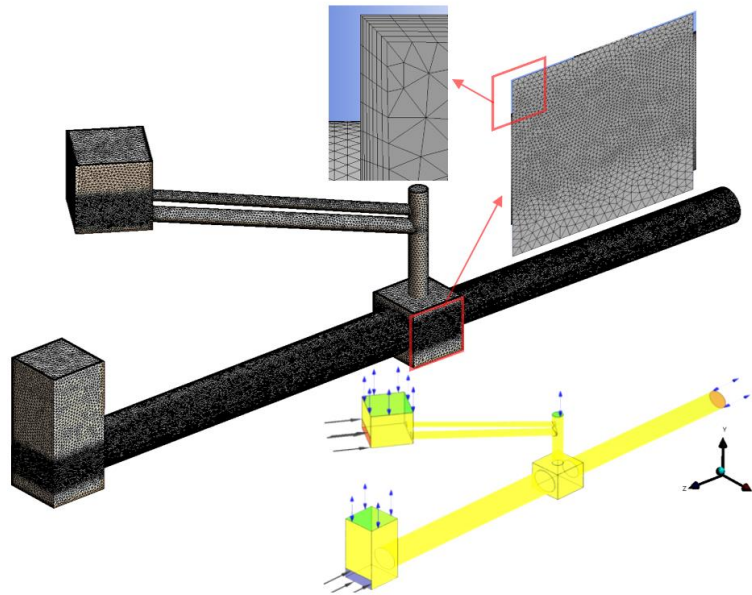


Figure 3. Meshed domain. Gravity force is considered in -Y direction. Bottom. Refinement and inflation as well as boundary conditions inside the domain are shown as insets

The mesh structure is assumed to be ideal if the skewness is less than 0.25 and orthogonality is close to 1.0. All fine mesh options have acceptable skewness and orthogonality (Table 4) [15]. Flow is subject to viscous effects near the walls where refinement of mesh size was performed. This was also applied where the free surface was anticipated to occur as shown in Figure 3. The coarse and medium mesh cases were unsatisfactory in terms of capturing gross flow parameters (Table 4). No detectable difference was observed in the free surface behaviour between options Fine 2 and 3. All three fine mesh options gave reliable results, but the Fine 2 option was accepted to be optimum by taking into consideration all relevant parameters, such as mesh skewness and run time (Table 4).

Time step, depended on Courant Number was defined as 0.1 seconds for an optimum solution which also matches the sampling frequency of the pressure sensor [14]. Regarding the relatively high Courant numbers in Table 4, the implicit transient code we utilize here does not require small Courant numbers for stability [16]. However, the optimized time step was chosen to reduce the RMS Courant number as much as possible. Mesh refining also helped obtain reasonable Courant numbers in the confined areas. This particularly helped resolve the unsteady behaviour of free fall.

Table 4. Mesh specifications for different mesh structures and comparisons of numerical model results with experimental model (EM) results. Bold columns indicate the chosen options

| Parameters | EM | C1 | C2 | M | F1 | F2 | F3 | k-ε | RNG | k-ω | SST |
|------------------------------------|------|--|-------|--------|--------|---------------|--------|---------------------------------|------|------|------|
| | | For different mesh structures (Coarse: C; Medium: M; Fine: F) | | | | | | For different turbulence models | | | |
| Element Number (x1000) | - | 338.9 | 528.7 | 1022.1 | 3000.5 | 5994.8 | 7861.4 | - | - | - | - |
| Node Number (x1000) | - | 114.4 | 172.9 | 309.9 | 781.7 | 1448.3 | 1886.9 | - | - | - | - |
| Skewness | - | 0.272 | 0.254 | 0.224 | 0.208 | 0.209 | 0.205 | - | - | - | - |
| Orthogonality Quality | - | 0.850 | 0.866 | 0.882 | 0.886 | 0.881 | 0.885 | - | - | - | - |
| RMS Courant Number | - | 12.57 | 21.73 | 10.28 | 11.86 | 13.40 | 13.87 | - | - | - | - |
| CPU Time (hour) | - | 01:38 | 02:01 | 03:53 | 12:20 | 20:15 | 34:11 | - | - | - | - |
| Averaged Pressure (Pa) | 856 | 937 | 928 | 950 | 950 | 925 | 923 | 950 | 926 | 909 | 941 |
| Q _{outlet} (l/s) | 2.71 | 2.97 | 2.92 | 2.89 | 2.78 | 2.61 | 2.58 | 2.78 | 2.63 | 2.81 | 2.89 |
| Averaged H _{Manhole} (mm) | 139 | 110 | 123 | 129 | 131 | 137 | 125 | 131 | 115 | 119 | 144 |
| H ₁ . Supply Tank (mm) | 128 | 104 | 113 | 115 | 120 | 125 | 115 | 120 | 106 | 119 | 138 |

In addition to mesh independency, different Reynolds Averaged Navier Stokes (RANS) turbulence closure models for 1.0-2.0 l/s discharge combinations were also tested. These models are k-epsilon (k-ε), re-normalisation group k-epsilon (RNG k-ε), k-omega (k-ω), k-omega shear stress transport (k-ω SST). Table 4 shows the results and comparison with experimental results. k-epsilon turbulence model was selected as the best option due to better agreement with experimental results, particularly for outlet discharge.

Boundary conditions are defined in the flow domain as shown in Figure 3. Sand grain roughness was defined on wall type boundary according to material properties. Mass flow type inlets are on the front surface of the first and second supply tanks. Allowing air to enter and exit, tops of the tanks were defined as opening type boundary. Pressure outlet was defined (0 Pa gage) at the end of the outlet pipe allowing water and air to exit and air to enter the domain. Discharge combinations from the experiments and design discharges were specified for each CFD model. Inlet water levels (head) were determined from experimental results.

Entire domain in the initialization of all runs were defined as air and stabilized conditions were obtained via long transient runs rather than adapting conditions from a preliminary steady run. This was in an effort not to dictate the flow depths and obtain realistic flow behaviour.

Convergence criteria was applied as follows. Three momentum equations and two turbulence equations (k-epsilon) were converged near 10^{-4} . Continuity equation was converged around 0.005 because of

stormwater retention in the domain (i.e. inlet and outlet discharges aren't always equal). Volume of Fluid (VOF) method was to resolve free surface.

14 out of 90 combinations from experimental work were selected for CFD modeling. Water level at the first supply tank and manhole were also compared at stable conditions. In the numerical model, stable condition was assumed when the outlet discharge reached stable (non-trending) conditions after about 60 seconds of simulation time. The stable values from the time steps near the end of the simulations were averaged from discharge-time series at the outlet surface. The same procedure was followed for water levels and local pressure values (similar to the treatment of the experimental data).

2.3.2. Validation

Table 5 shows comparisons of local pressure values for five discharge combinations. Given the 1% or less error for the majority of the runs, the validation using the local pressure values is satisfactory. Table 3 also shows comparison of outlet discharges for 14 discharge combinations as a second validation. Big majority are within an error margin of 10% and less which is acceptable. Water levels in the manhole and the first supply tank were compared for the same 14 discharge combinations (Table 5) which gave lower error margins despite the high turbulence intensity near that region. Water levels in the first supply tank however were not matched very closely (error near 10%). This is presumably due to the deficiencies of the VOF method and/or air-water mix capabilities of RANS based transient simulation. Also both the free surface and boundedness requirements are believed to be causing the larger error margin in discharge compared to pressure.

Table 5. Comparisons between experimental (EM) and numerical modelling (NM) for each discharge combination (DC) along with the error (E)

| DC (l/s) | EM (l/s) | NM (l/s) | E (%) | EM (mm) | NM (mm) | E (%) | EM (mm) | NM (mm) | E (%) | EM (Pa) | NM (Pa) | E (%) |
|--|-------------|-------------|--|------------|------------|--|------------|------------|------------------|------------|------------|----------|
| Outlet Discharge comparison for each discharge combination | | | Water level comparisons in the manhole | | | Water level comparisons in the first supply tank | | | Average Pressure | | | |
| 0.1-0.1 | 0.19 | 0.18 | -5.3 | 65 | 62 | -4.6 | 59 | 54 | -8.5 | 760 | 765 | 0.7 |
| 0.1-2.0 | 1.82 | 1.74 | -4.4 | 130 | 119 | -8.5 | 106 | 98 | -7.6 | 856 | 925 | 8.0 |
| 0.5-1.0 | 1.22 | 1.39 | 14.0 | 98 | 95 | -3.1 | 96 | 97 | 1.0 | - | - | - |
| 0.5-1.5 | 1.74 | 1.79 | 2.9 | 116 | 115 | -0.9 | 105 | 98 | -6.7 | - | - | - |
| 1.0-1.0 | 1.75 | 1.88 | 7.4 | 108 | 104 | -3.7 | 108 | 99 | -8.3 | - | - | - |
| 1.0-2.0 | 2.71 | 2.61 | -3.7 | 139 | 137 | -1.4 | 128 | 125 | -2.3 | - | - | - |
| 1.8-0.5 | 2.15 | 2.23 | 8.4 | 109 | 111 | 1.8 | 119 | 109 | -8.4 | - | - | - |
| 1.8-1.8 | 3.08 | 3.09 | 0.3 | 138 | 138 | 0.0 | 139 | 130 | -6.5 | - | - | - |
| 2.0-0.8 | 2.41 | 2.66 | 10.4 | 114 | 116 | 1.8 | 131 | 113 | -13.7 | 871 | 862 | -1.1 |
| 2.0-1.0 | 2.67 | 2.70 | 1.1 | 126 | 123 | -2.4 | 131 | 119 | -9.2 | - | - | - |
| 2.5-0.1 | 2.20 | 2.46 | 11.8 | 109 | 106 | -2.8 | 135 | 123 | -8.9 | - | - | - |
| 2.5-0.8 | 2.86 | 3.19 | 11.5 | 125 | 120 | -4.0 | 140 | 127 | -9.3 | 953 | 933 | -2.1 |
| 2.5-1.0 | 3.03 | 3.31 | 9.2 | 129 | 126 | -2.3 | 142 | 137 | -3.5 | 974 | 968 | -0.6 |
| 2.5-2.0 | 4.17 | 3.79 | -9.1 | 157 | 151 | -3.8 | 158 | 144 | -8.9 | - | - | - |

3. RESULTS AND DISCUSSION

3.1. Investigation of the Original System

With the acceptable validation, the CFD model was subsequently used to investigate the performance of the system using design and maximum capacity discharges. Another goal here was to identify the systems problem once again using the numerical model.

First, the supply tanks were removed from the domain. Pipe's input discharge was determined according to Manning's equation as given in the regulations [17] to be 13.61 l/s. Outlet pipe's design discharge is 15.52 l/s. Secondary corrugated pipe's design discharges are 4.93 and 1.39 l/s. Outlet pipe's discharge capacity is high because of the high slope. Stormwater system should ideally deliver no more than 90% of the design capacity according to the regulations. 90% operating condition also represents the maximum filling conditions for this system. In the CFD model, both 100% and 90% usage were considered. Possible operational problems were: (i) possibilities of overflow through the manhole cover, (ii) outlet discharge being equal to total inlet discharge and (iii) exceeding water levels at 90% along the main pipes. The inlet boundary conditions were fixed to represent 90% fullness at initialization. Fair, Geyer and Okun [17] formed a diagram based on Manning's equation to help designers obtain gross flow parameters using the degree of fullness or vice versa at a given section, which was used here.

Next, the structure was tested numerically without adding secondary pipes to the manhole. It was observed in this case that the system didn't have overflow or backflow problems. The first supply tank was added to the system again in order to show the backflow effect (Figure 4). It is understood that the secondary pipes are the main cause of the backflow. Nevertheless, adding the secondary pipes was inevitable for the authorities because the accumulated stormwater must be discharged in that new area.

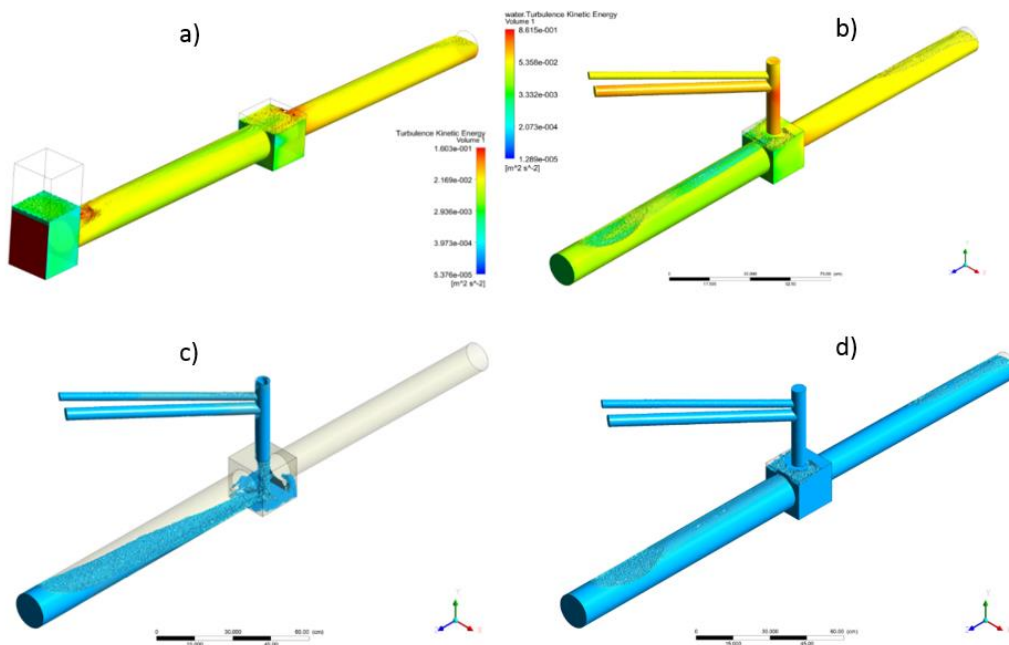


Figure 4. CFD model results: a) turbulence kinetic energy (TKE) without the manhole and secondary pipes, b) TKE with the manhole and secondary pipes (TKE parameter was used to colour the water volume fraction to help assess the level of mixing at a given domain), c) fast overflow in the manhole for 100% using conditions, d) the filled domain with storm water for 100% using conditions

The following results are for 100% using conditions. The outlet discharge reached 16.75 l/s within 2 seconds and became stable while it should be 15.51 l/s according to Manning’s equation. This result makes the standards in the regulation questionable for this particular storm water structure. CFD results also show the overflow discharge from the manhole to be 2.05 l/s while it should be “0” according to the regulations. This overflow shown in Figure 4 was also observed in the physical model tests.

3.2. Implications for Remedial Measures

In an effort to provide solution to the overflow and backflow problems, three new manhole geometries were designed and are shown in Figure 5. They were tested with full and 90% capacity discharges focusing on increasing manhole’s outlet discharge capacity and decreasing the turbulence level in the manhole. The latter is a measure of the water mix due to drop of water into the manhole.

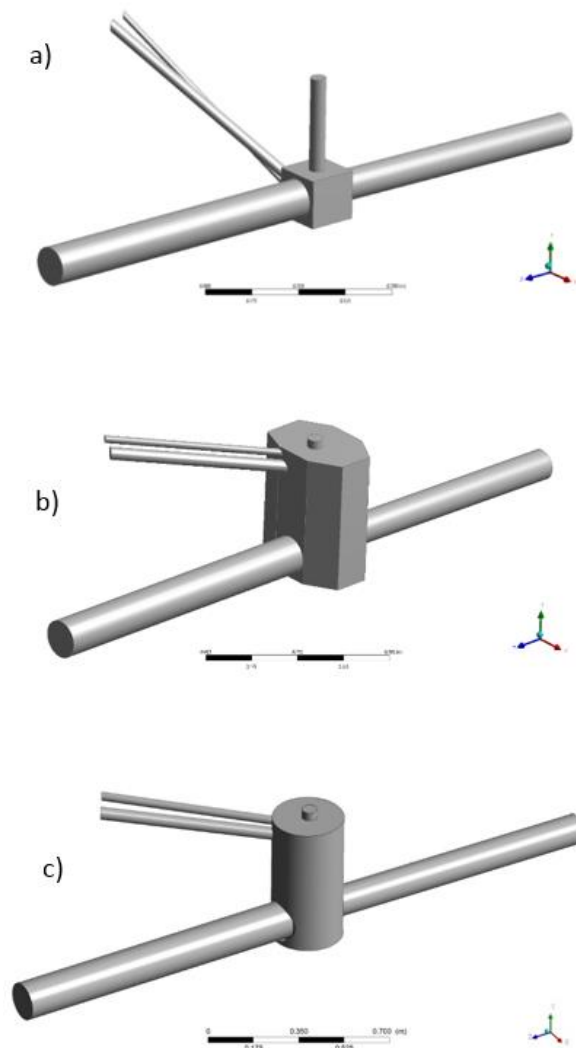


Figure 5. Three new geometry improvements: (a) alternative 1; (b) alternative 2; (c) alternative 3

In the first design, slopes of secondary corrugated pipes were directly integrated to the same manhole (Figure 5a). Although secondary pipe’s discharges were changed according to Manning equation (because the slope changed), overflow suddenly occurred in the manhole (Figure 6). In fact, the important one is original discharges, because they were obtained from a hydrological study. The first

alternative is found to be preventing the overflow. Water level is fixed at 225 mm in the manhole as shown in Figure 6b. Nevertheless, the new slopes of the secondary pipes exceed the acceptable levels in the regulations. High slopes also cause high velocity and turbulence in the manhole.

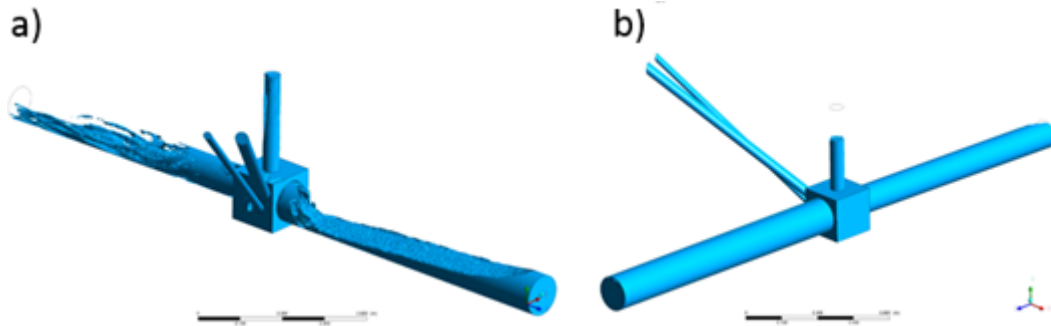


Figure 6. Alternative 1: Fast overflow for new discharges in the manhole (a) and operating condition with previous discharges (b)

Second design is intended to increase the manhole’s volume for retention with the hexagonal geometry (Figure 5b, 525 mm high and 160 mm for each edge). Slopes and discharges remained the same for all pipes. Upper side of the manhole was kept the same as the original. Second alternative can easily discharge entered stormwater from the system as shown in Figure 7. This condition uses maximum discharges from Manning equation for all pipes (worst-case scenario). Although the sharp sides contribute to the mixing, the higher volume is then enough to decrease the mixing level. This alternative was also tested for normal operating conditions (also called minimum condition in the regulation, Figure 7b) and it is a potential solution although not economical.

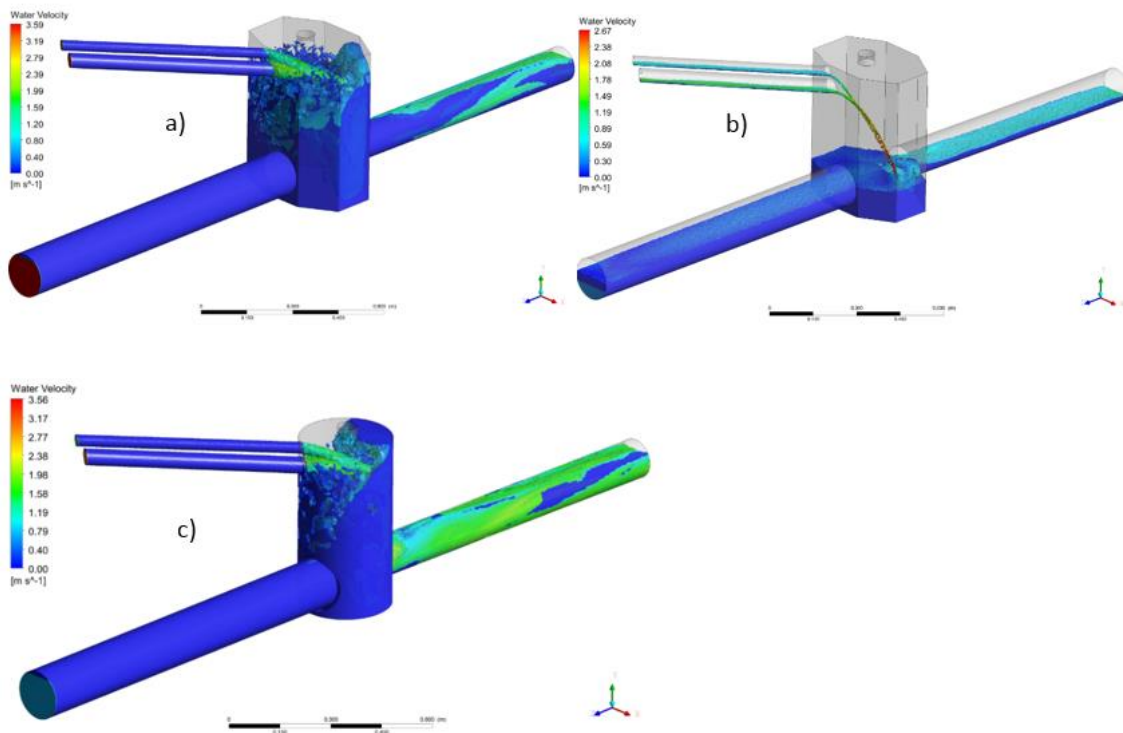


Figure 7. Alternative 2 in maximum operating condition (a); and in minimum operating condition (b); alternative 3 in maximum operating condition (c), all with water velocity rendering the volume fraction

Third design is a larger circular manhole (Figure 5c, 525 mm high and 280 mm in diameter). It is not only increasing the manhole's volume for retention using a simpler and more practical geometry, but also aiming to decrease the mixing level in the manhole. Figure 7c shows that third alternative easily discharges the storm water from the system in maximum operating conditions. Maximum water velocity profiles are almost the same with alternative two. Hence, it can be said that the circular and larger tank is a better solution.

All CFD models presented here indicate that the water levels in the pipes are below 90% even though the discharges are 90% of the operating conditions. Figure 8 shows the water levels in the pipes for alternatives 2 and 3.

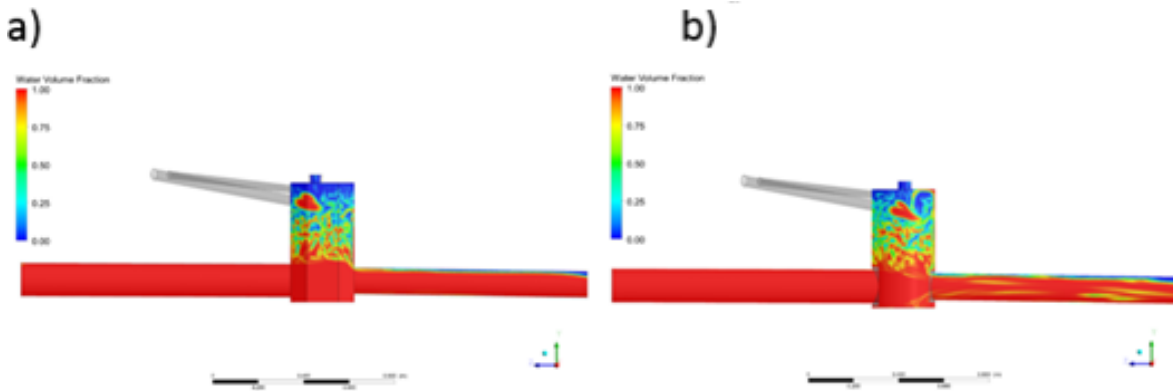


Figure 8. Water volume fraction for Alternative 2 (a) and Alternative 3 (b)

4. CONCLUSIONS

An existing and problematic stormwater drainage system was investigated using experimental and numerical modelling. Firstly, 1:10 scaled physical model was used to investigate the system experimentally. For the RANS based transient CFD models, mesh independency and comparison of turbulence models were performed. CFD model was successfully validated with experimental results in terms of pressure, outlet discharge and water levels. Overflow and backflow were observed in the system in both experiments and CFD models. High turbulence and mixing in the manhole as a result of secondary pipes is the cause of the backflow in the system. This is proved by observing that the outlet discharge is less than the total inlet discharges under design conditions. CFD model showed that outlet discharges and water levels are not always in agreement with the design values based on the regulations and Manning's equation. Therefore, conventional approaches fail to detect the problem and also are not useful in finding a solution. Three new manholes were designed and tested with the validated CFD model with alternative 3 selected to be the more suitable solution.

In light of the above discussion, with proper validation, CFD model is shown to be a powerful and effective tool for investigating, designing or rehabilitating stormwater drainage systems. Particularly, unconventional solutions to complex problems in such systems, where the empirical approaches fail to characterize, can be realized, tested and modified with less time and cost compared to experimental or field work.

ACKNOWLEDGEMENTS

Datasets for this research are included in this thesis: “Investigation of Stormwater Drainage Systems with Experimental and Numerical Methods”, (Yilmazer C. 2019). Also CFD model files or code that support the findings of this study are available from the corresponding author upon reasonable request. There is no funding source.

CONFLICT OF INTEREST

The authors stated that there are no conflicts of interest regarding the publication of this article.

AUTHORSHIP CONTRIBUTIONS

Cem Yilmazer: Experimental and numerical modeling, Methodology, Visualization, Writing – original draft. **Ahmet Ozan Çelik:** Supervision, Writing – review & editing.

REFERENCES

- [1] Saiyudthong C, Guymer I. Simulation of energy loss due to changes in pipe direction across a manhole. 10th National Conference on Civil Engineering 2005; 5-9.
- [2] Zhao CH, Zhu DZ, Rajaratnam N. Computational and experimental study of surcharged flow at a 90 combining sewer junction. *J Hydraul Eng* 2008; 134(6): 688-700.
- [3] Sousa V, Meireles I, Matos J, Almeida MC. Numerical modelling of air-water flow in a vertical drop manhole. 7th International Conference on Sewer Processes and Networks, 2013.
- [4] Beg NA, Carvalho RF, Lopes P, Leandro J, Melo N. Numerical investigation of the flow field inside a manhole-pipe drainage system. 6th International Symposium on Hydraulic Structures, 2016.
- [5] Motlagh YY, Nazemi AH, Sadraddini AA, Abbaspour A, Motlagh SY. Numerical investigation of the effects of combining sewer junction characteristics on the hydraulic parameters of flow in fully surcharged condition. *Water Environ J* 2013; 27(3): 301-316.
- [6] Chen Z, Han S, Zhou FY, Wang K. A CFD modeling approach for municipal sewer system design optimization to minimize emissions into receiving water body. *Water Resour Manag* 2013; 27: 2053-2069.
- [7] Isel S, Dufresne M, Bardiaux JB, Fischer M, Vazquez J. Computational fluid dynamics based assessment of discharge-water depth relationships for combined sewer overflows. *Urban Water J* 2014; 11(8): 631-640.
- [8] Kaur K, Laanearu J, Annus I. Numerical study of Tallinn storm-water system flooding conditions using CFD simulations of multi-phase flow in a large-scale inverted siphon. *IOP Conf. Ser.: Mater. Sci. Eng.* 2017; 251: 121-128.
- [9] Beg NA, Carvalho RF, Leandro J. Comparison of flow hydraulics in different manhole types. *Proceedings of the 37th IAHR World Congress* 2017; 6865: 4212-4221.

- [10] Özölçer IH, Dündar O. Determination of energy loss coefficient of rainwater and sewer manholes with CFD. *Fresenius Environ Bull* 2017; 26(7): 4716-4725.
- [11] Beg NA, Carvalho RF, Leandro J. Effect of surcharge on gully-manhole flow. *J. Hydro-Environ Res* 2018; 19: 224-236.
- [12] Wang J, Vasconcelos JG. Manhole cover displacement caused by the release of entrapped air pockets. *J Water Manag Model* 2018; 26(444): 1-6.
- [13] Beg NA, Carvalho RF, Leandro J. Effect of manhole molds and inlet alignment on the hydraulics of circular manhole at changing surcharge. *Urban Water J* 2019; 16(1): 33-44.
- [14] Yilmazer C. Investigation of Stormwater Drainage Systems with Experimental and Numerical Methods. MSc, Eskişehir Technical University, Eskişehir, Turkey, 2019.
- [15] Ansys Inc. ANSYS meshing user's guide. Canonsburg, PA, USA: 2010.
- [16] Ansys Inc. ANSYS CFX – Pre User's Guide, Release 15. Canonsburg, PA, USA: 2013.
- [17] Fair GM, Geyer JC, Okun DA. Elements of Water Supply and Wastewater Disposal. John Wiley & Sons 1971.